Highly-Efficiency Low-*AR* Aerial Vehicles in Urban Transit

Galen J. Suppes, PhD, P.E.
Chief Engineer
HS-Drone, LLC
Charlottesville, VA 22911
Email: gjsuppes@gmail.com

Adam B. Suppes, PhD
Senior Research Engineer
HS-Drone, LLC
Charlottesville, VA 22911
Email: suppesadam@yahoo.com

Word Count: 7,006 words + 1 table

Submitted July 31, 2023
Revised and Resubmitted November 27, 2023.
Posted 12/3/23

ABSTRACT

The economics of UAM operations is highly dependent on the flight efficiency of airframes (L/D-Efficiency), with many recent AAM transition VTOL prototypes reducing the gap in L/D-Efficiency between rotary and fixed-wing aircraft. Higher Efficiency for transitional VTOL ***L/D*** will become the new norm; however, the wide wingspans for efficient airframes are inconsistent with mobility within urban infrastructure. The challenge is to achieve high L/D-Efficiency in low ***AR*** airframes. When that challenge is met, common vehicles can be used toward quicker and lower-cost transit in converging technologies of fixed-wing aircraft, rotary-wing aircraft, aerial guideway systems, and regional transit.

This paper uses CFD simulations to advance insight into design guidelines that enable low ***AR*** airframes to achieve ***L/D*** in excess of 20 and ultimately 40 (versus 17 for typical airliners). These advances are enabled due to the convergence of several factors including: a) improved heuristic-level insight into lifting-body design and b) distributed propulsion with electric powered aircraft. Transit times and costs may be reduced by 70% to 90% with huge economic impacts including significant mitigation of greenhouse gas emissions.

The following abbreviated terms apply: UAM - Urban Air Mobility, AAM - Advanced Air Mobility, VTOL - Vertical Takeoff and Landing, ***AR*** - Aspect Ratio, defined as the span divided by the longitudinal chord length, CFD - Computational Fluid Dynamics, ***L/D*** - lift-drag ratio, the primary measure of L/D-Efficiency, AoA – Air's angle of attack.

Key Words: vertiport, airfoil, CFD, aspect ratio, airframe, urban, unmanned, hyperloop, guideway

INTRODUCTION

In recent years, the fuel efficiency per revenue-passenger kilometer (RPK-Efficiency) has approximately doubled every two decades[1] with airliner transit rivaling rail transit, both with RPK-Efficiencies greater than automobiles and buses. With the advent of basic economy airfares, flights frequently cost less than the transit to and from airports, both in time and expense—especially when airport and TSA fees are removed from ticket costs. This alone identifies that a significant advance in access to aerial transit would have an economic impact approaching that of the world's current air transit sector, about $900 billion per year.

Replacing both air transit and airport access with a single system would have an economic impact of well over a trillion dollars per year. With electric propulsion, there exists the opportunity for reduced greenhouse gas emissions, improved safety, national energy security, and reduced maintenance costs.

Wide wingspans, as traditionally necessary for efficient air transit, inhibit access between buildings throughout inner city and urban regions. A high-L/D-Efficiency, low ***AR*** airframe could provide access similar to automobiles without the burden of locating parking spaces; these UAM systems will favor low-turnaround-time autonomous air taxis over private vehicles. Such low ***AR*** aerial vehicles could follow zipline-type guideways through dense traffic areas with smooth transition of flight to or from the guideway. In this approach, intracity mass transit and inter-city aerial vehicles would share guideways with advantages of reduced overall infrastructure cost and improved access.

An aircraft's lift-drag ratio (***L/D***) characterizes the aircraft's energy L/D-Efficiency; high ***L/D*** have traditionally been attained with wide wingspans consistent with high Aspect-Ratio (***AR***) aircraft. Benchmark ***L/D*** include 21 (B2 Bomber), 21 (Nasa's Pathfinder Plus), 56 (ASH 31 glider with an ***AR*** of 33.5), 70 (Eta motor glider with an ***AR*** of 51), 22-25 (typical HAPS/HALE aircraft),[2, 3] and 16-18 (typical airliners like the B737 with an ***AR*** from 9 to 10). For comparison, helicopters have an ***L/D*** of 5-7, and multicopters, including quadcopters, tend to have ***L/D*** less than helicopters.

These benchmarks identify that a transitional VTOL can take ***L/D*** from about 5 to about 10 for urban operation. Targeted ***L/D*** for the airframes of this project are >20 for initial smaller drone systems and up to 40 for larger scales. These targets are for scalable airframes with ***AR*** between 0.5 and 2.0.

Increased L/D-Efficiency in an aircraft allows fuel and battery weights to be replaced with payload, further improving RPK-Efficiency. The results are airframes at 1.5-8X the L/D-Efficiency of

contemporary counterparts with larger increases for RPK-Efficiency. These factors are calculated from the benchmarks listed above. Such drastic advances are rare.

For electric aircraft, L/D-Efficiency is particularly important since increased L/D-Efficiency drastically increases the aircraft capabilities under battery, solar,[4] and hybrid power. By the year 2025, the U.S. department of energy projects solar panel costs will be at 1 ¢/kWh [4, 5 6] versus diesel fuel costs at 18 ¢/kWh. This can translate to over 90% reduction in energy costs. Additional benefits of electric propulsion include: a) robustness, b) low maintenance, c) zero point-source emissions, d) scalability, e) compatibility with zero-greenhouse-gas-emission sources of energy, f) synergy with distributed propulsion, and g) general ease of use.

While modern airliners are achieving improved RPK-Efficiency by using fewer higher-bypass-ratio turbojet engines, distributed propulsion approaches use additional smaller motors. The robust nature of electric motors and easy distribution of electrical power makes distributed propulsion viable. One benefit of distributed propulsion is the creation of an array of thrust sources that can create balanced and redundant VTOL capabilities. CFD studies can quantify the benefits of distributed propulsion toward enabling high L/D-Efficiency in low ***AR*** designs.

Accurate heuristics are needed to guide the design process. The first subsection of the RESULTS uses CFD to identify these heuristics which are summarized in Table 1. The remainder of the INTRODUCTION identifies the flaws of paradigms that currently dominate the industry along.

Heuristics in Aircraft Design

The most common explanation of aerodynamic flight is Bernoulli's theory of flight, which has persisted for decades as part of education programs in engineering, science, engineering technology, and flight schools. Bernoulli's equation is derived from an energy balance on a system under the assumption of an incompressible fluid and identifies how pressure, velocity, and fluid height relate to work input or output. Decades after its derivation, the equation was applied to estimate aerodynamic lift under the inaccurate assumption that air takes the same amount of time to travel from the leading edge to the trailing edge of a wing over/under the upper and lower wing surfaces; whereby, a larger distance of travel on the upper surface results in higher velocities with lower resultant pressures. It is inaccurate to assume that air takes the same time to travel leading-to-trailing edge over different surfaces. It is also inaccurate to assume that air's velocity gradients in boundary layers are accurately characterized by single velocities—an additional assumption of the theory. The negative impact of having an incorrect prominent explanation of flight has stifled aircraft innovations that deviate from prominent tube-and-wing designs; however, detailed engineering of aircraft designs is a refined and respected art typically using CFD.

A common alternative theory is the "momentum theory of lift", which has an accurate derivation in its characterization of how a propulsion sources provide thrust through Newton's second law. This thrust may be in any direction, including vertical to change the altitude of a vehicle. It is useful for estimating energy needed for changes in altitude and velocity. However, for steady-state flight without change in altitude, there is no vertical force through a distance. Thus, the momentum theory of lift is ultimately inaccurate, or useless, at the limit of zero altitude change during steady-state flight.

Aerodynamic flight is fundamentally based on air flows which create higher pressures on lower surfaces and lower pressures on upper surfaces (cumulatively, "lift-pressures"). Table 1 summarizes airframe design heuristics identified using CFD results presented in the RESULTS of this paper:

The designs of this work target ***L/D*** starting at 20:1 for low ***AR*** designs. Longer-term goals are 40:1 with refinement of the approaches presented herein. To achieve these efficiencies, the prominent lift-generating surfaces need to be at angles less than 1.5° from horizontal. Therefore, the design of highly efficient aircraft has the strategic targets of: 1) high pressure sources on lower surfaces, 2) low pressure sources on upper surfaces, and 3) the expansion of those pressure source bubbles on surfaces less than 1° from horizontal. Neither the Bernoulli theory of lift nor the momentum theory of flight identifies these strategic targets, nor do they address design guidelines toward achieving higher ***L/D.***

Table 1. Heuristics on designing to create aerodynamic lift and flight efficiency.

For Airfoils (2D cross-sections):

- **A-1.** Air's velocity impacting a surface generates higher pressure.
- **A-2.** Air's velocity diverging from a surface generates lower pressure.
- **A-3.** Air expands at speed of sound from high-to-low pressure (except within boundary layer).
- **A-4.** Air's velocity bends toward lower pressure and away from higher pressure.
- **A-5.** A surface's ***L/D*** is the normalized surface integral of Pressure $\tan^{-1}(\alpha)$ on the surface, per:

$$Lift = \Delta P\ \Delta S\ Cos(\alpha_P); \quad Drag_{form} = \Delta P\ \Delta S\ Sin(\alpha_P);$$
$$L/D = \frac{1}{Tan(\alpha_P)} = \frac{57}{\alpha_P^{\circ}}\ at\ low\ \alpha_P \qquad (1)$$

- **A-6.** Shear forces are negligible at $C_d > 0.01$; $C_{d,\,shear} < 0.001$ for smooth surfaces.

For the addition of Sources (propulsors like jets, propellers, and fans):

- **S-1.** Increasing Source power increases Lift at trailing edge of Lift Spans[1]; when Lift Span pitch angle < 0° from horizontal, Source power increases ***L/D*** as limited by the Operating Point.
- **S-2.** For ***L/D*** > 40, induced thrust is necessary; induced thrust counteracts Drag.
- **S-3.** For the highest L/D: the Lift Span, Nose, and (optional) wings need to have pitches coordinated with Lift Span interaction with a Source.
- **S-4.** High induced Drag on surfaces > 3° should be eliminated by transforming pressure to near free stream pressures.
- **S-5.** A mid-chord Source can propagate lower pressure forward to increase overall ***L/D.***
- **S-6.** Optimal Lift Span pitches decrease with increasing Source power.

For Wings (i.e. 3D airfoils):

- **W-1.** Lift pressures are lost over side edges of a wing (2D airfoils do not have side-edge losses).
- **W-2.** Use camber, fences, and distributed Sources to compensate for lost Lift pressure.
- **W-3.** High ***AR*** wings may be added to low ***AR*** lifting bodies to increase ***L/D.***
- **W-4.** Wing loadings vary with application, approximately: Military jets (700 kg/m^2, with C_L of 1.5), commercial jets (300-500, 1.5-1.6), commercial prop aircraft (100-200, 0.8), prop drones (50, 0.5)C, and HAPS/HALE (2-7, <0.4). When essentially all the planform generates lift, $C_L = [m\ g] / [\rho\ A\ u^2]$. Where at a planform loading of 2, $C_L = 2\ g / [\rho\ u^2]$. At 80 m/s and 0.1 kg/m^3 $C_L = 0.03$ (i.e., HAPS aircraft have much lower C_L needs than jets).

An artifact of aircraft design based on inaccurate heuristics is the prominence of either tube-and-wing or flying wing designs. Both of these designs tend to achieve maximum ***L/D*** near 23:1; a "local" optimum. Good, detailed engineering is applied to these local optima designs, while other design optimums have gone undetected—a classic pitfall in the science of optimization.

CFD has emerged as an accurate and useful simulation tool to optimize designs; CFD results provide a basis to form rules of thumb (i.e., heuristics) on aircraft design. Good heuristics coalesce trends of complex physical phenomena into a few guidelines that the human mind can simultaneously consider to produce-base case designs and improvements.

Identifying good heuristics is an objective of the research summarized in this paper. An additional objective is identifying high-speed low-***AR*** airframes having ***L/D*** > 20 in designs that expand the capabilities of solar-powered aircraft.

METHODS

This paper benefits from over three decades of innovation documenting a progression of concepts; starting with hyperloop type approaches documented over two decades before Elon Musk revitalized such approaches. By example, maglev suspension is unnecessary since aerodynamic lift forces are sufficient to generate aerodynamic lift at high speeds. A tethered glider system uses

[1] Lift span is the term used to describe a surface in front of a propulsor where low intake pressures induce Lift.

inexpensive zipline-type guideways, [7] but early concepts were flawed because low ***AR*** vehicles had poor ***L/D.*** [8]

In 2019, the burst of activity on rotary aircraft, ***L/D*** around 5, dominated air taxi system design; this provided motivation to identify an improved transformer/hybrid VTOL design. In 2021, the transformer VTOL designs expanded to include platform aircraft with high surface areas for solar panels. Identified markets extended to HAPS/HALE and new applications of 24/7 stratospheric platforms: the stratosphere was identified as a new frontier with opportunities for improved manufacturing, communications, and bases of operation. In this 30-years of concept evolution, the common theme of the need for high ***L/D*** low ***AR*** aircraft emerged.

Parallel to concept advancement, 500-gram scale remote-control prototypes of transformer VTOL and aerial platform aircraft advanced critical approaches to takeoff and landing as well as approaches to control surfaces. In January of 2023, CFD studies were initiated to improve designs. These studies rapidly identified distributed propulsion as vital to the optimization of high ***L/D*** low ***AR*** designs. The CFD studies also provided insight into aerodynamic lift that resulted in the primary design heuristics of Table 1.

CFD studies were performed using parameters as recommended by Simflow and Open Foam software. [9, 10] Visualization of results was performed in Paraview. Unless otherwise stated, the free stream velocity for CFD results are 40 m/s in air at 1 bar pressure.

RESULTS

Understanding Aerodynamic Lift

Figure 1 pressure profiles of a vertically-symmetric airfoil and its asymmetric variations illustrate how lift pressure regions are created on surfaces by aerodynamic forces. Proceeding from the leading edge to the trailing edge on the symmetric airfoil at zero pitch (Fig. 1a): a) air at free stream velocity impacts the leading edge to create a high pressure bubble; b) a low pressure area forms behind the leading edge bubble as the result of the expansion of that bubble with a velocity vector that diverges from the surface; c) the resulting low pressure region ultimately bends air back towards the surface, resulting in an increase in pressure behind the lowest pressure region, d) subsequent air flow balances the tendency for air to flow straight/parallel versus bending to follow surface curves, and e) behind the trailing edge, velocity streams from upper and lower surfaces collide to create a region of higher pressure.

When the surface of the airfoil is flat, air eventually achieves a flow parallel to the surface and pressure approaches the free stream

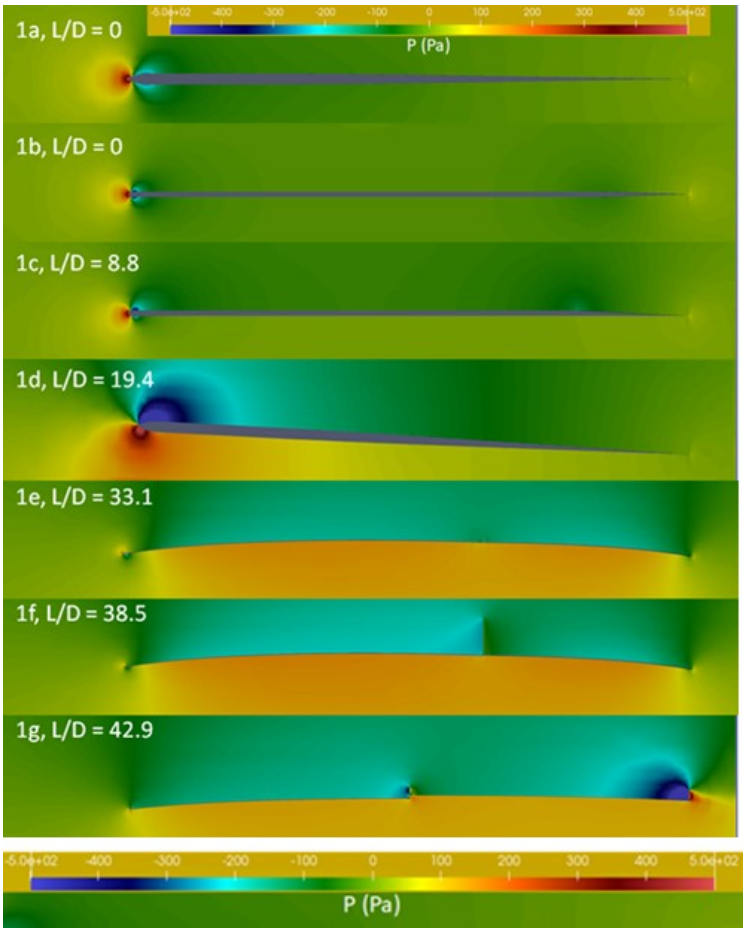

Figure 1. Pressure profiles on airfoils that illustrate key aspects of how to generate aerodynamic lift.

value until the surface tapers to the trailing edge point (see Fig. 1b). An asymmetry in the trailing section taper (Fig. 1c) results in the formation of a trailing-section low-pressure region—that low-pressure bubble impacts pressure throughout the airfoil, producing an increase in ***L/D*** from 0 to 8.8. Air expands at the speed of sound, which overcomes oncoming velocity in subsonic flight.

Fig. 1d illustrates how a change in airfoil pitch causes more air to diverge from upper surfaces and more air to converge on lower surfaces to create lift; increased pitch creates more lift at the lower velocities of takeoff and landing. While ***L/D*** is typically not a strong function of velocity, the lift and drag coefficients and forces can be strong functions of velocity.

When at sufficient magnitude, the lower-pressure bubble draws air from afore and below the leading edge; this changes air's angle of attack ("AoA") at the leading-edge, moving the leading-edge higher-pressure bubble rearwards towards more-horizontal surfaces. This transformation is a key feature of airfoils achieving ***L/D*** greater than 40:1. Ultra-high ***L/D*** requires reduced drag, versus increased lift; reduced drag occurs when induced thrust at the leading-edge cancels the drag of the remaining airfoil surfaces.

A disadvantage of using airfoil pitch to generate greater lift is the resulting increase in surface area with surface pitch angles greater than 2°, resulting in a lower ***L/D.*** This geometric constraint is discussed in the next subsection.

In addition to using curved surfaces and overall pitch to create lift pressures, propulsion sources ("Sources") can create lift pressures. Use of Sources to control pressures on lifting body surfaces is an aspect of distributed propulsion. Fig. 1f illustrates how a Source at about 0.7 c (70% back along the chord) on the upper surface can produce an area of low pressure that extends forward.

A Source at the upper surface's trailing edge simultaneously increases lift pressures on both upper and lower surfaces (see Fig. 1g).

In compatible configurations, the ***L/D*** will continue to increase with increasing Source power; however, horizontal surfaces in front of a Source can choke airflow into the Source, thereby reducing the efficiency of thrust generation. Desirably, more power is saved due to reduced drag than is lost due to choking the Source. A detailed study of this ratio identifies that the ratio of reduced drag to reduced thrust can exceed 10X. The take-away is that correctly applied distributed propulsion can significantly improve L/D-Efficiency with the detailed experimental studies being outside the scope of this paper.

Impact of Surface's Angle Relative to Horizontal

During steady-state flight, the lift for an airplane is equal to the weight. The drag is thus equal to the weight of the aircraft divided by ***L/D.*** The power needed for steady-state flight is drag times velocity.

Under the definition of "form drag" as the drag created by pressure at the surface, total drag is the sum of form and shear drag. The same surface pressure creates both lift and form drag. The form drag of a differential surface area is the product of the pressure (ΔP) at the surface (ΔS) times the horizontal component of the surface normal vector (Sin($\boldsymbol{\alpha}$)) of the force generated by that pressure. For a flat surface neglecting edge effects, no further assumptions are necessary to derive ***L/D*** per Equation 1:

$$Lift = \Delta P\, \Delta S\, Cos(\alpha); \quad Drag_{form} = \Delta P\, \Delta S\, Sin(\alpha); \quad L/D = \frac{1}{Tan(\alpha)} = \frac{57}{\alpha^\circ} \ at\ low\ \alpha \qquad (1)$$

where ΔP at the is the pressure at the surface less the free stream pressure. ***L/D*** > 57 can be achieved through a prominence of lift pressures on surfaces at α < 1°; however, typically ***L/D*** > 57 are achieved by inducing thrust which decreases the denominator of Equation 1, which is not accounted for by Equation 1. The ***L/D*** values of Fig. 1 illustrate the following aspects of this axiom:

- Fig. 1d illustrates how the lowest lower-pressure region remains around the horizontal peak of the airfoil. This dynamic feature is what has made contemporary airfoil designs the cornerstone of wing design; an evenly distributed pressure profile would lead to much lower ***L/D.***
- Fig. 1e illustrates a substantially evenly-distributed pressure profile on a thin cambered airfoil. For a thin-cambered airfoil, the higher values of α in trailing sections are compensated for by negative values of α (aka, induced thrust) near the leading edge.

- Fig. 1g illustrates a highest value of ***L/D*** due to a propulsion source developing desired higher and lower pressures around both the leading and trailing edges.

A simple flat plate airfoil can be placed at a position where entire surface is essentially at the desired angle; however, air will flow parallel to the surface shortly after the leading edge. That parallel air flow has neither impacting nor diverging components to create lift pressures (see Fig. 1b).

Lift pressures may be created by:

a) a curvature of a surfaces causing air to impact or diverge from that surface,
b) a [propulsion] Source, and
c) a flap.

The lift pressures generated by these means will expand at the speed of sound and interact with the direction of otherwise free stream velocity near the surface. These guidelines are summarized by Table 1 and are demonstrated by the pressure profiles of Figure 1.

Applications to Low *AR* Lifting Bodies

A high ***L/D*** for the airfoil (i.e., cross sections of a wing or lifting body) is a necessary but not sufficient condition for a high ***L/D*** wing or lifting body. The lift-generating pressures (i.e., higher pressures on lower surfaces and lower pressures on upper surfaces) can dissipate laterally, over the side edges; that lateral dissipation is not accounted-for in 2-D simulations.

Equation 2 is a lifting-line theory derivation that accounts for dissipation of lift pressures over side edges.

$$C_d = \frac{C_l^2}{\pi AR\, e} \tag{2}$$

where $\boldsymbol{C_d}$ is the drag coefficient, $\boldsymbol{C_l}$ is the lift coefficient, and $\boldsymbol{e}$ is an L/D-Efficiency factor.

Wings of elliptical planform and sword point ends were the earliest method to mitigate side-edge dissipation. Contemporary airliners typically incorporate winglets which have vertical components that block side-edge dissipation. Winglets can be in excess of eight feet high which is 13.3% of a 120 ft wingspan.

To mitigate lift dissipation across side edges that are longer than an aircraft is wide require a fence rather than a winglet. However, an eight-foot fence height on a 16 ft wingspan is impractical both from the weight and drag perspectives. Distributed propulsion provides an alternative solution. The following are advantages of distributed propulsion long-chord side-edges of a lifting body span:

- Incremental and repeatable increases in ***L/D*** due to the Source intake above the surface and exhaust below the surface—Sources can compensate for dissipation losses.
- At the Source, surface pitches can be changed, allowing more near-horizontal surfaces for lift pressures; this overcomes constraints for the need for increasing curvature and respective surface angles of longer-chord surfaces; it allows the formation of a "train" of solar panels.
- The equivalent of jet-wash velocity streams trends reduces the residence time for lift pressures to dissipate over side edges.

An optimal configuration of the mid-chord distributed propulsion intakes from the upper surface and discharges below lower surfaces, both with horizontal (or near-horizontal) vector trajectories.

The optimization of dissipation mitigation deployment includes optimizing the following parameters:

- Size and locations of distributed propulsion along the edge.
- Size and locations of winglets or fences to complement the distributed propulsion array.
- Power settings of distributed propulsion array to reduce drag at constant lift—settings that cause greater drag reduction than lift reduction.

Solving the respective multi-parameter optimization is beyond the scope of this instant text.

3D CFD Studies

3D CFD studies are necessary to account for side dissipation losses and dissipation mitigation. Figure 2 illustrates various configurations with thin cambered wings and distributed propulsion.

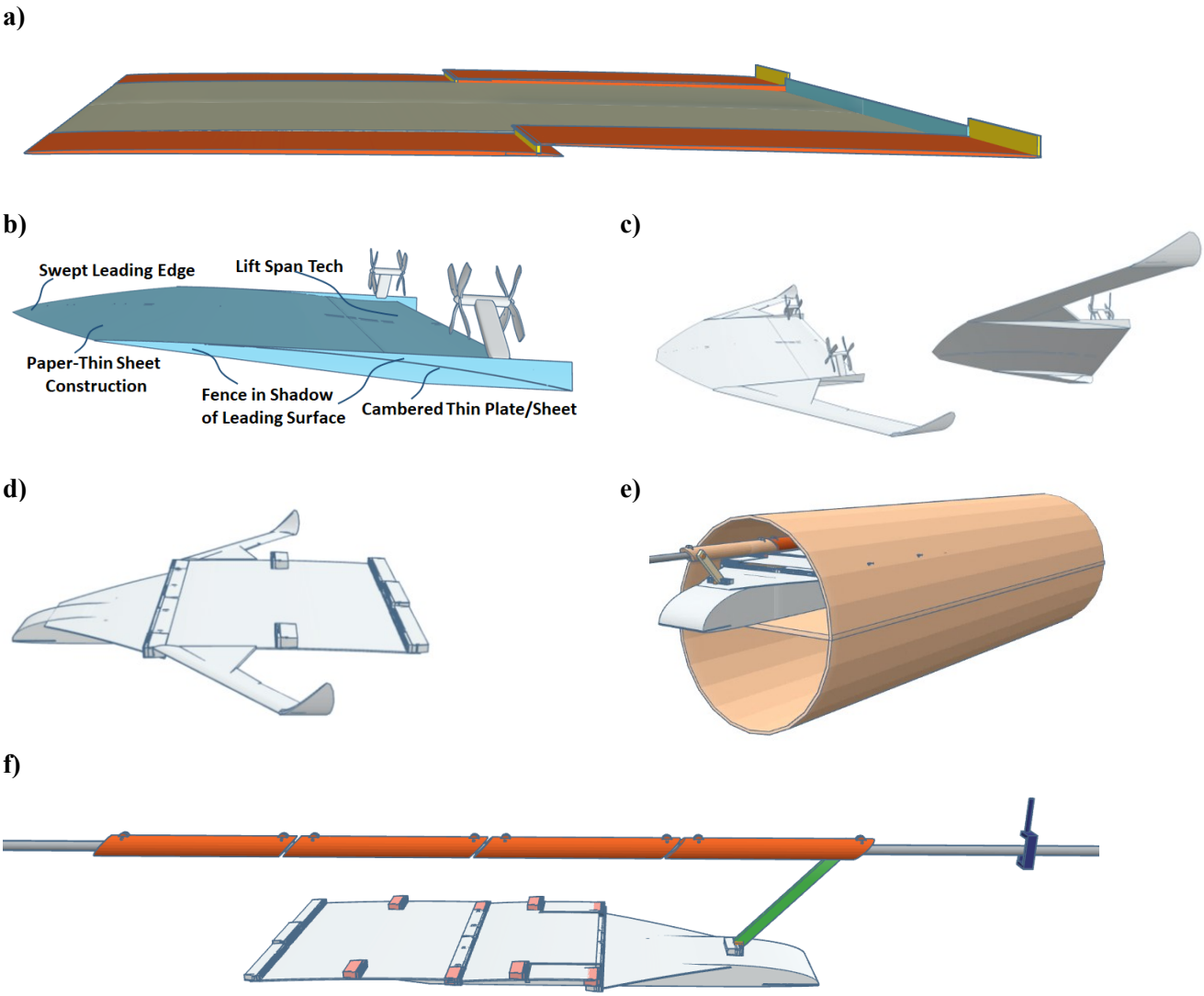

Figure 2. STL images of thin cambered wing designs with distributed propulsion and illustrating: a) an STL file for CFD simulation, b) a thin cambered center wing design, c) a thin cambered center wing with side wing extensions, d) a thin cambered center wing with side wing extensions and fuselage, e) a tunnel configuration, and f) a tethered guideway configuration.

The design presented in Figure 2a. is: a main body middle section with split airfoil side sections incorporating distributed propulsion. Key features are:

a) The main body is a thin wing at low camber enabling the potential for good performance as illustrated by Fig. 1e.
b) The side airfoil is two thin cambered wing sections in sequence similar to the airfoil of Fig. 1g, including Sources between the two sections and at the trailing edge.

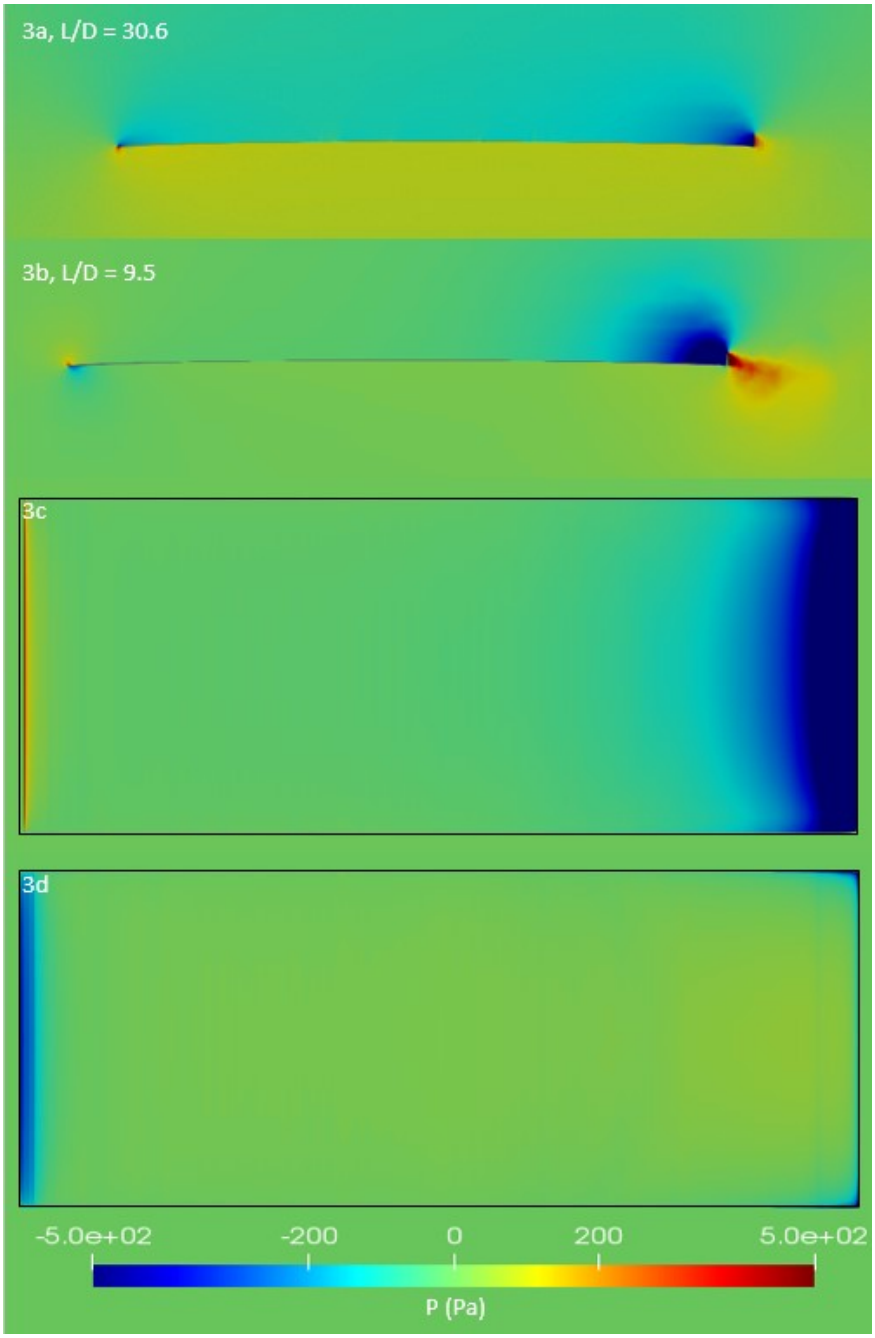

Figure 3. 2D (3a) and 3D CFD (3b-3d, *AR*=0.4) pressure profiles of thin cambered wing with rear propulsion.

c) Tunable parameters for a symmetric design include: a) three wing section cambers; b) mid-chord Sources' height, width, location, and power setting, and c) trailing edge Sources' height, width, and power settings.

The middle and side sections of the Figure 2a wing were evaluated in 3D CFD simulation as the middle section alone at ***AR*** = 0.4 (Figure 3), the side sections alone at ***AR*** = 0.6 (Figure 4a-d), and with both middle and side section at ***AR*** = 0.6 (Figure 4e-h). The 3D simulations identify a significant decrease in ***L/D*** versus the ideal airfoil sections of the 2D simulations.

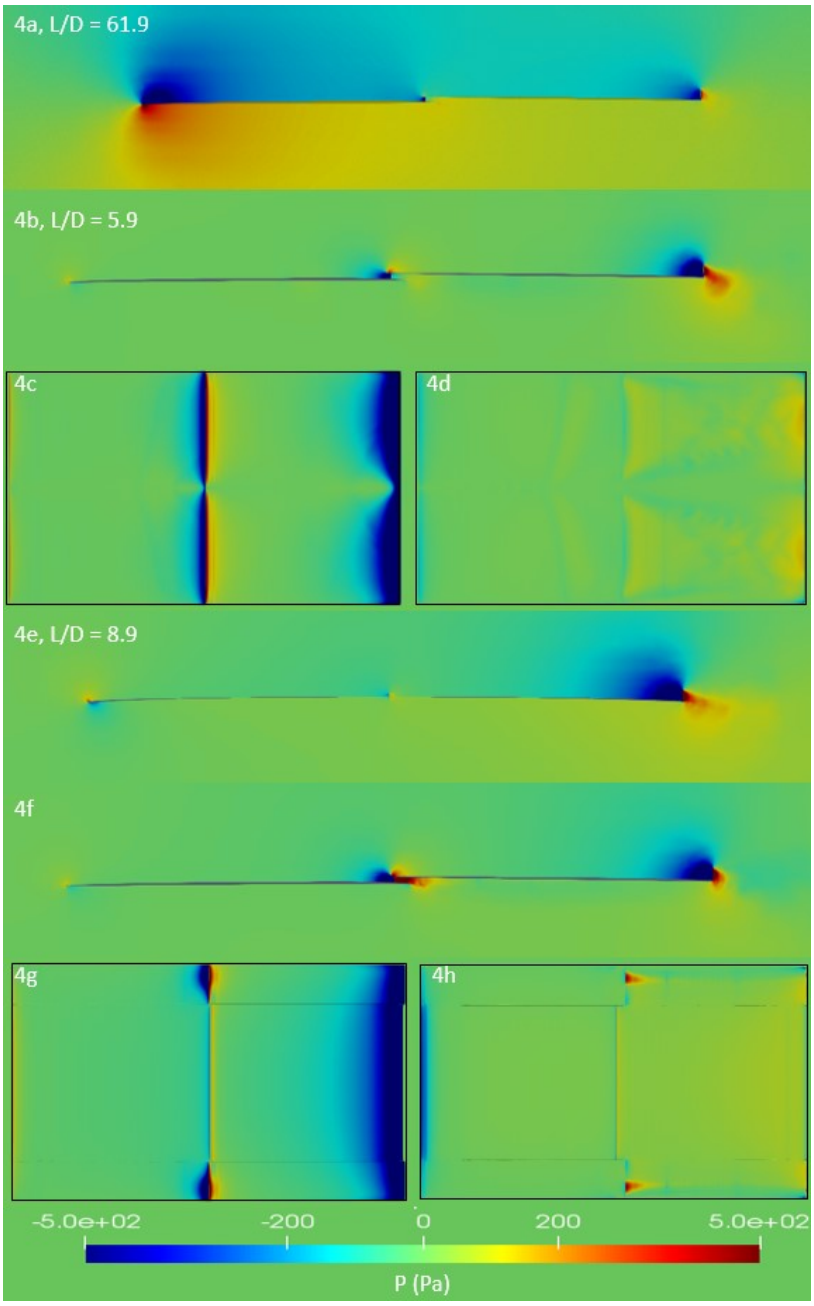

Figure 4. 2D (4a) and 3D CFD (4b-4d, 4e-4h, *AR*=0.6) pressure profiles airfoils having mid-chord Sources with intake above a leading wing section and exhaust below the trailing wing section.

Figure 5 data identify trends of ***L/D*** versus ***AR*** for 3D wings. The only data point transferred from Figure 3 and 4 to Figure 5 is the 0.4 ***AR*** point at 9.5 ***L/D*** from Figure 3; other data points were from additional CFD simulations. The close proximity of the Equation 2 line (black) and the control lines (Sources turned off, blue & Orange) substantiate a good veracity of the CFD simulations per agreement with Equation 2.

Turning on the Sources results in significant increases in ***L/D***, validating the use of Sources to overcome deterioration caused by side and trailing edge dissipation.

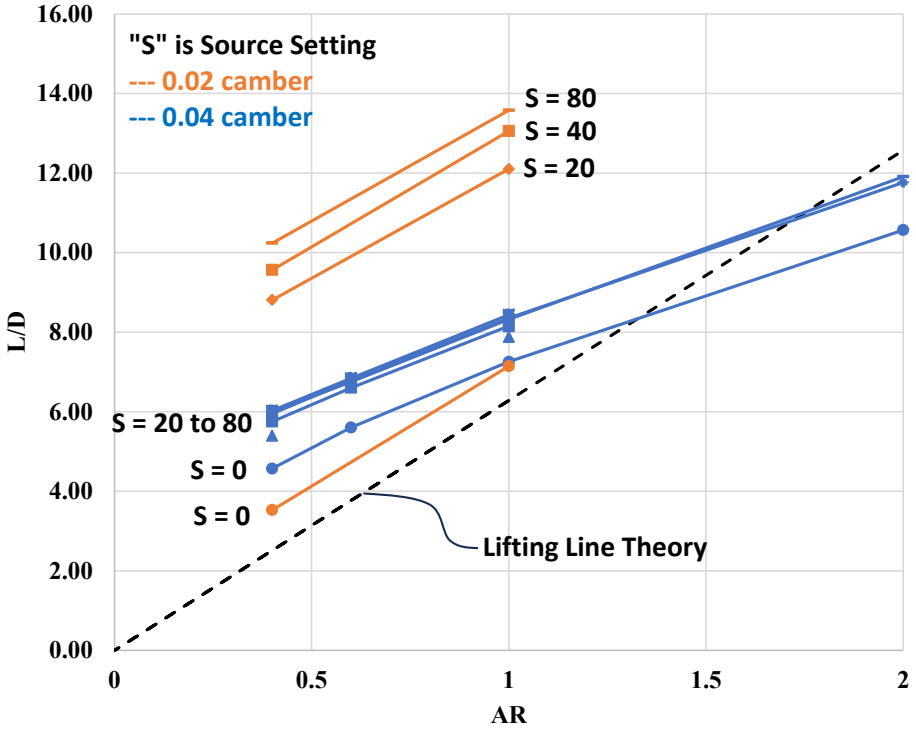

Figure 5. Impact of *AR*, Sources, and camber on *L/D* for thin cambered airfoils.

DISCUSSION

Effectiveness of Distributed Propulsion to Mitigate Dissipation Losses

Clearly, distributed propulsion is an effective tool to mitigate dissipation-related losses and design high ***L/D*** low ***AR*** airframes. The results of Figure 5 provide a proof of concept with the following takeaway bullets:

- 3D simulations agree with the Equation 2, the ***AR*** equation, in the limit without Sources.
- Sources are effective in mitigating edge dissipation losses.
- Low ***AR*** dissipation losses for ***L/D*** supersede high airfoil ***L/D*** in wing performance (i.e., performance is a strong function of ***AR***).

Degrees of freedom to overcome dissipation formation in wings include:

1. size, location, and power of Sources;
2. size and shape of winglets/fences;
3. combinations of wing sections including sectioning and overall ***AR***;
4. use of delta wing leading sections; and
5. pitch angles of the entire airframe as well as local pitch angles created by surface camber.

Complete optimization will require supercomputers to consider the many degrees of freedom. It is suggested that these designs will meet an initial goal of ***L/D*** = 20 at ***AR*** = 1.0 with higher values at greater ***AR*** and the addition of wing extensions outside a thin central section.

Additional heuristics, as summarized by Table 1, emerge as a result of studying the impact of sources and distributed propulsion; three as repeated here are:

S-4. High induced Drag on surfaces > 3° should be eliminated by transforming pressure to near free stream pressures or transforming surface through addition of induced thrust.

S-5. A mid-chord Source can propagate lower pressure forward to increase overall ***L/D.***

S-6. Optimal Lift Span pitches decrease with increasing Source power.

Blended wing body designs have lateral with extensions which block side-edge losses from a thick central wing, similar wing extensions can be used to overcome dissipation of the Figure 5 thin center wings.

Iconic Wing Tip Vortex Formation

Characterizing a trailing wing tip vortex as creating drag is inaccurate, since no part of the object's surface exists within the iconic wing tip vortex. Rather, an edge vortex is a visualization of lost work associated with higher pressure air below the wing going around the tip to lower pressure air above the wing. The relevant optimization target is reducing loss of lift pressures at the surfaces rather than a focus on the vortex beyond a wing tip.

A vortex can form when a thin surface at a side edge separate significant upper-surface pressures that are lower than free stream pressures and significant lower surface pressures that are higher than free stream pressures. Simulations of this work have shown that the prominent loss of lift across side edges is due to dissipation to free stream regions rather than a vortex flow between upper and lower surfaces.

Solar Power with Distributed Electrical Propulsion Augmentation to High Speed and Jet Transit

Solar power options create a synergetic nexus with increasing ***L/D*** efficiencies, where:

- L/D-efficiency leverages the use of solar power and enhances electric propulsion.
- Direct solar power reduces battery and fuel weights.
- Electric propulsion enables distributed propulsion.
- Distributed propulsion enables higher ***L/D*** efficiencies.

When considering hybrid electric-fuel propulsion, this nexus and cycle expand to include:

- Solar and battery power provide alternative energy and power for emergencies,
- Alternative emergency propulsion allows jet engines to be reduced in number to a single jet engine for an aircraft while being able to meet safety standards.
- Reduced jet engines reduce weights and costs.

When considering temporal effects:

- Solar power costs will continue to decrease in costs and increase in efficiency.
- Higher amounts of reflected sunlight above the clouds, versus reflected light a few feet above Earth's surface, enable bifacial plates to attain productivities.
- Decreasing weight of solar power (i.e., thin cambered wings) increases excess power for higher speeds and the general ability to generate excess power toward an expanding range of applications.

Figure 6 illustrates different types of solar aircraft in regions of velocity versus weight space showing contemporary 24/7 solar (yellow) and direct solar regions of operation (green). Towed panel technology and increased ***L/D*** expand both regions towards and including smaller regional aircraft passenger services. Manufacturing platforms, carriers, and refueler regions are identified; they would be unable to routinely takeoff and land due to extended solar arrays. The two hybrid aircraft regions would require fuel and/or battery augmentation.

For Type-1 hybrid aircraft, over half the power is from solar energy and battery power with all-electric propulsion service for all but long-haul markets. As the aircraft weight increases to the Type-2 Hybrid region, at least one fuel-powered jet engine is required to sustain the combinations of higher velocities and heavier weights.

Advantages for Type-2 Hybrid systems that can significantly reduce transit costs include:

- Electric propulsion is the major supplemental power source for takeoff, landing, and attaining altitude, during which velocities are lower than cruising velocities.
- Electric propulsion is a failsafe backup for a single-jet-engine design.
- Electric propulsion is a premium power that can be distributed and leveraged to reduce drag.

This approach identifies liquid fuels as having the advantage to increase velocity and electric distributed propulsion as strategic in increasing ***L/D***, decreasing cost, and improving safety. In this strategic application of distributed propulsion, solar power can replace over half the fuel consumption with significant reductions in costs by increasing payload and eliminating redundant jet engines. A low-***AR*** distributed-propulsion aircraft is adaptable to configurations for vertical takeoff, including large passenger airliners.

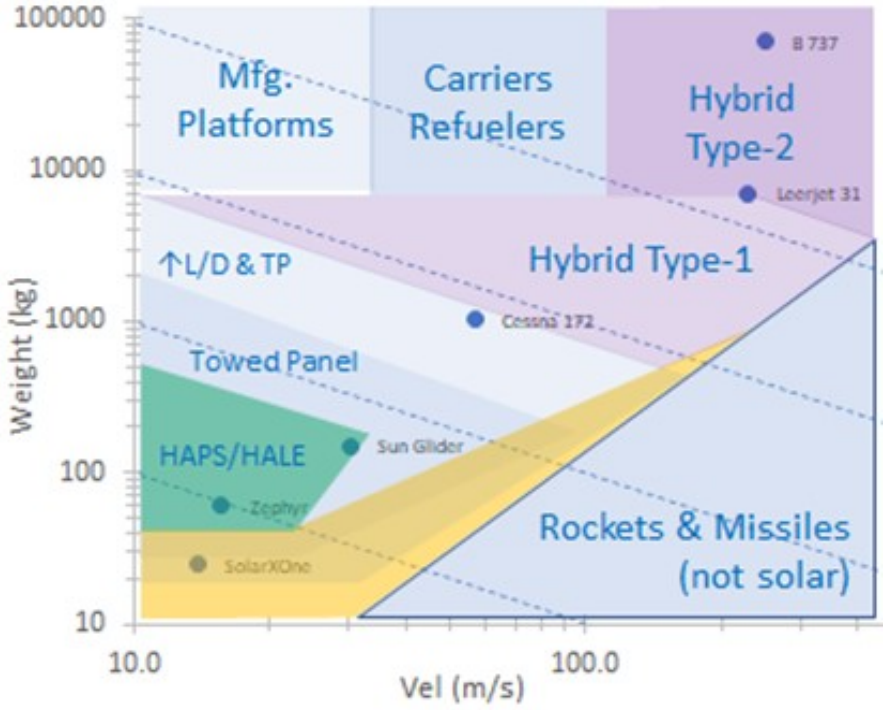

Figure 6. Illustration of different types of solar aircraft as enabled with high *L/D* low *AR* airframes.

Converging of Vertiport, Regional Transit, and Mass Transit

Tethered glider guideway systems include decades-old concepts that have failed to materialize due to the width of the corridor necessary to accommodate the wide wingspans of aircraft being assisted by guideway tethers. Low ***AR*** airframes with high ***L/D*** overcome this historic obstacle and have increasing viability on use with low-cost low-environmental-impact zipline guideways.

A low ***AR*** aircraft with a high ***L/D*** (i.e., in excess of 20) could be configured for transition to and from vertical takeoff. That aircraft may be configured to operate along a zipline-type [aerial] guideway within urban infrastructure with the optional ability to disconnect from that guideway. In this design, air taxis (i.e., vertiport), mass transit, and long-distance airliners become increasingly indistinguishable.

In this approach, the "vertiport" is not a single port, but rather, a zipline transit network within cities where vehicles are released for free flight outside no-fly zones. A serious obstacle to air taxis as a new standard of transportation is the air traffic regulations over populated areas and restricted air spaces. A "zipline transit network vertiport" is a governable solution to this obstacle.

As illustrated by Figure 2e, high ***L/D*** low ***AR*** designs can fly in tunnels, such as in hyperloop-type corridors. Figure 7 illustrates an approach for open access of vehicles to and from hyperloop-type tubes. This technology bridges the gap between hyperloop, guideway, aerial transit, and veritports. It substantially reduces the cost and timeline for implementing hyperloop-type systems and impacts the overall optimization of the converged economic sectors.

Vehicles traveling in a tube will impart a velocity to the air in the tube, even at low pressures. That velocity created by moving vessels is the driving force for the counter-current convective mass transfer of the Bernoulli loops of Figure 7. The driving force for convective flow is represented by the upper and lower lines of the graph of Figure 7; these lines include dynamic pressure corrections which the Bernoulli tubes convert to practical driving forces for mass transfer.

The concept of operating with large tunnel entrances and exits open to the surroundings can be disturbing; however, when the pressure change is distributed over 1-10 miles, the driving force for air

flow (ΔP/ΔL) is low. Optimal tube operating pressures would be steady-state conditions that passively adjust with traffic volume.

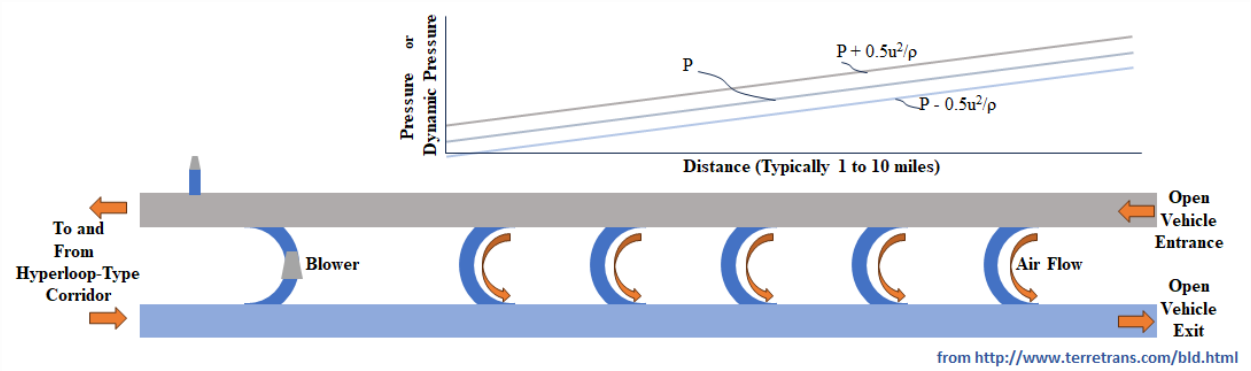

Figure 7. Bernoulli loops of low-pressure hyperloop-type tunnels allowing vehicles to enter and exit from atmospheric surroundings. Borrowed with permission from http://www.terretrans.com/bld.html.

Many hyperloop approaches are problematic in the manner that tunnel corridor pressures are treated as a specification rather than an optimization variable. A phenomenon that greatly impacts this optimization is the impact of pressure on ***L/D.***

Under the assumption that shear drag can be neglected relative to form drag, the impact of pressure on ***L/D*** cancels since the same pressure creates both lift and drag. For an aircraft that is substantially a lifting body, pressure and altitude have little impact on L/D-Efficiency. The approximation loses accuracy as less of the airframe is a lifting body, such as a tube-and-wing airframes. To achieve ***L/D*** >40, nearly every surface of the aircraft needs to generate lift. This becomes more complicated for low ***AR*** designs, yet there remain many degrees of freedom and large areas of R&D to be investigated (e.g., use of distributed Sources to increase ***L/D***).

Aerial Vehicle Zipline Transit versus Contemporary Trains

Trains are designed to minimize form drag as the result of a streamlined design where shear drag becomes dominant. Transit in shear-dominant regimes is substantially harder with a train using primarily aerodynamic lift since side edge dissipation losses result in loss of lift along the length of the train and must be compensated-for by periodic distributed propulsion embodiments. A comparison of the advantages of each is revealing.

Advantages of Aerial Vehicle Guideways include:

- The absence of a carriage below the passenger compartment reduces both shear and form drag.
- A greater distance from the ground creates less shear drag.
- Greater flat upper-surface areas allow for collection of more solar energy.
- Non-contact lift reduces maintenance costs.
- Standard use of non-contact propulsion reduces maintenance costs.
- Vehicles may leave guideway to routes without roads or guideways.
- Lower costs for guideways.
- Reduced environmental impact where the infrastructure footprint is posts every quarter to half mile increments versus a track corridor.
- A synergy with concurrent regional distribution of electrical power and communication cables.
- Improved compatibility with smaller-vehicle branches for freight and parcel shipment.

- Improved options for high-speed and low-lead-time switching operations that enable more non-stop service and faster transit times.
- Higher speeds and reduced transit times increase passenger turnover.

Advantages of Contemporary Trains include:

- Absence of a need for distributed propulsion with associated form drag losses along the length of the train.
- Lower cost penalty for incremental addition of weight such as in sleeper cars and cafeterias.
- Access to current guideway infrastructure.

For lower-traffic regional corridors that use shorter trains, the zipline system emerges as superior. For short-term profitability, tapping into existing rail lines has advantages unless the current system is not self-sustaining without government subsidies. Once corridors of zipline-type transit are in place, aerial transit systems will have advantages in reduced expansion and maintenance costs. Also, in applications with significant solar energy at the surface (i.e., U.S. Southwest with minimal cloud cover and reliably lengthy daylight hour), aerial transit has advantages over rail.

Broader Impact

Figures 2a-c illustrate thin cambered airfoil applications of distributed propulsion to reduce side-edge dissipation losses. The objective is to achieve a low ***AR*** aerial vehicle with high ***L/D.*** This design promotes the prominent use of lift-generating surfaces <1° from horizontal where lower-angle surfaces are operated to provide induced thrust. The maximum amount of induced thrust at the leading edge is dependent on a number of factors including velocity and the ability to orient surfaces at the nose of the vehicle to maximize induced thrust and ***L/D.***

Figures 4a, 4d, and 4f illustrate thin cambered panel sections trailing a lead section. Distributed propulsion at the transitions between panels resolves interference issues and allows the resetting of the surface pitches to <1° from horizontal. This allows for the extension of a train of cambered solar panels. Calculations show that each solar panel in a light-weight thin-camber design at ***L/D*** > 10 (10 for bifacial panel, 20 for mono-facial panel) is able to produce >4X the energy needed to sustain that panel's 24/7 flight. [13] Hence, these solar panels are a self-sustaining power source for 24/7 aircraft of purposes beyond applications of contemporary aircraft. Such applications include airborne aircraft carriers and manufacturing platforms for chemicals such as hydrogen and ammonia.

Within the timeframe of the implementation of this technology, the DOE projects the cost of solar panels to be 1 ¢/kWh versus aviation fuel costs at 18 ¢/kWh.[5-6] The average U.S. grid electricity costs about 16¢/kWh. For aerial manufacturing platforms, the transit routes are a degree of freedom. This creates the opportunity to operate without sunset at the poles or to operate with velocity with the earth's rotation at night. This has an impact of reducing the "annualized" cost of solar panels as less than <0.8¢/kWh with reduced need for the 24/7 aircraft to use part of the energy for piercing the night time darkness. Especially at highly-reflective surfaces of the poles, solar panels can collect both direct and reflected sunlight. In the 10-year timeframe, the cost of electric power for these 24/7 towed solar panels should be <0.5¢/kWh.

The Greatest Barrier to New Transit Technologies

Typically, the greatest barrier to new transformative transit technologies is the way infrastructure of established technologies can overwhelm the 2-5 year profitability for using existing infrastructure versus building new infrastructure. Hence, for half a century, the innovation power of the U.S. has been dominated by incremental rather than transformative advances.

Low ***AR*** high ***L/D*** aerial vehicles enable bridging technologies that can link most of subsonic aircraft, mass transit, and hyperloop applications attainable with incremental advances from initial applications of these low ***AR*** high ***L/D*** aerial vehicles.

When a bridging technology creates a continuous design parameter field between two historically-distinct technologies, the technologies converge with the prospect of new performance optima. This suggests that optimal designs in historically-distinct technologies are local optima with the true overall optima in the converged economic sector.

Technology that transforms rotary-wing airframes to fixed-wing airframes is an example of such a bridging. Low Aspect ratio fixed wing airframes with distributed propulsion is a bridging technology, and when the new aircraft have the access of VTOL with the L/D-Efficiency of fixed-wing, new optima emerge that eliminate the time and energy associated with transport to and from transportation hubs.

The following is a summary of bridging technologies presented in this paper:

- High ***L/D*** low ***AR*** airframes enabled by distributed propulsion and thin camber airfoils bridging rotary-wing to fixed-wing airframe sectors.
- Zipline-type guided aerial vehicle guideways that allow vehicles to attach to or leave the guideway bridging rail transit sectors.
- Bernoulli-Loop entrances to and from pressure-controlled tunnel transit corridors bridging hyperloop-type systems with rail transit systems including mass transit. [11, 14]
- Solar Towed Platform technology bridging the gaps between contemporary solar aircraft, satellites, fuel production (e.g. hydrogen), chemical production (e.g. ammonia), deployed fleets (e.g. aircraft carrier fleets, naval fleets), and space launch platforms (i.e., improved access to orbit and space).

Bridging technologies converge respective economic sectors, or subsectors, examples mentioned by the above bullets. Impacted economic sectors go beyond the aforementioned, including agriculture and tourism, since vehicles and platforms have many uses in these sectors. In view of the prospects that half-mile-spaced structures supporting zipline-type transit corridors could provide preferred commercial and residential sites, the technology also bridges the gap to construction and energy distribution sectors. A radical reduction in the cost and time of transit has significant ramifications on health care and education economic sectors.

The high ***L/D*** as described and summarized in this paper enable significant reductions in energies consumed by these economic sectors and enable opportunities for major greenhouse gas emission mitigation, pointing toward new overall optima in designs throughout the bridged sectors.

The embodiments of this paper have a patent-pending status with the entirety of the first draft of the paper submitted in a provisional patent application. [15]

CONCLUSIONS

High ***L/D*** low ***AR*** airframes can merge the gap between transit systems characterized as vertiport, mass transit, hyperloop, regional air, long-haul air, HAPS/HALE, and aerial drone technologies. High ***L/D*** is an L/D-Efficiency metric, and low ***AR*** enables access in congested urban areas that are inaccessible with wide wingspans. A synergetic nexus emerges where high ***L/D*** enables electric propulsion, thin cambered wings enable bifacial solar power which reduces battery and fuel weights and costs, electric propulsion enables distributed propulsion, and distributed propulsion enables high ***L/D*** in low ***AR*** airframe designs. This new category of airframe technology is validated by CFD simulations where the path of innovation is guided by this paper's Table 1 heuristics.

ACKNOWLEDGMENTS

This work was made possible by the Suppes Family Trust with primary contributor Kimberly Suppes, MD.

AUTHOR CONTRIBUTIONS

The authors confirm contribution to the paper as follows: study conception, design, editing, 2D CFD simulations, and interpretation of 2D simulation results: G.J. Suppes; 2D and 3D CFD simulations, interpretation of CFD results, related information technology, and editing: A.B. Suppes

REFERENCES

1 Energy efficiency in transport. (2023). Retrieved from https://en.wikipedia.org/w/index.php?title=Energy_efficiency_in_transport&oldid=1144848549#cite_note-ORNL/TM-2020/1770-135.

2 Moelyadi, M. A., & Zulkarnain, M. F. (2021). HALE UAV ITB perpetual flight. *IOP Conference Series: Materials Science and Engineering, 1109*(1).

3 Peck, A. (2020, -12-28). HAPS/HALE: Seeking solar's sweet spot. *Inside Unmanned Systems,* Retrieved from https://insideunmannedsystems.com/haps-hale-seeking-solars-sweet-spot/.

4 Solar energy diagram. (2011). Retrieved from http://solarenergyfactsblog.com/solar-energy-diagram/.

5 Breaking down solar farm costs: Free template inside — RatedPower. (2021). Retrieved from https://ratedpower.com/blog/solar-farm-costs/.

6 Solar Energy Technologies Office.2030 solar cost targets. Retrieved from https://www.energy.gov/eere/solar/articles/2030-solar-cost-targets..

7 Suppes, G. (2019). In The Suppes Family Trust (Ed.), *Terreplane transportation system* . US.

8 Suppes, G.*Perspective on maglev transit and introduction of personal rapid transit maglev.* (). Retrieved from https://onlinepubs.trb.org/Onlinepubs/trr/1995/1496/1496-013.pdf.

9 Airfoil (NACA 0012) tutorial - SimFlow CFD software. Retrieved from https://help.sim-flow.com/tutorials/airfoil-naca-0012.

10 Wing tutorial - SimFlow CFD software. Retrieved from https://help.sim-flow.com/tutorials/wing.

11 Korn, J. (2022). Alice, the first all-electric passenger airplane, takes flight | CNN business. Retrieved from https://www.cnn.com/2022/09/27/tech/eviation-alice-first-flight/index.html.

12 Singh, H. (2022). Cae launches electric aircraft modification program with piper aircraft. Retrieved from https://www.aviation-defence-universe.com/cae-launches-electric-aircraft-modification-program-with-piper-aircraft-inc/.

13 Power ratio calculations. Retrieved from https://www.weebly.com/editor/main.php#/.

14 Davis, S.C., Boundy, R.G. (2022). *Transportation energy data book* (Edition 40 ed.) Oak Ridge National Laboratory. Retrieved from https://tedb.ornl.gov/wp-content/uploads/2022/03/TEDB_Ed_40.pdf.

15 Patent portfolio. Retrieved from http://www.terretrans.com/tech.html, 2023 (Jul 31,),